Accepted to the International Journal of Robotics and Computer-Integrated Manufacturing, May 1988.

Symbolic Modeling and Dynamic Simulation of Robotic Manipulators with Compliant Links and Joints

Dr. Sabri Cetinkunt
Assistant Professor
Dept. of Mechanical Engineering
University of Illinois at Chicago
Chicago, IL 60680

Dr. Wayne J. Book
Professor
The George W. Woodruff School of
Mechanical Engineering
Georgia Institute of Technology
Atlanta, GA 30332

Abstract

The explicit, non-recursive symbolic form of the dynamic model of robotic manipulators with compliant links and joints are developed based on Lagrangian- assumed modes formulation. This form of dynamic model is suitable for controller synthesis, as well as accurate simulations of robotic applications. The final form of the equations are organized in a form similar to rigid manipulator equations. This allows one to identify the differences between rigid and flexible manipulator dynamics explicitly. Therefore, current knowledge on control of rigid manipulators is likely to be utilized in a maximum way in developing new control algorithms for flexible manipulators.

Computer automated symbolic expansion of the dynamic model equations for any desired manipulator is accomplished with programs written based on commercial symbolic manipulation programs (SMP, MACSYMA, REDUCE). A two-link manipulator is used as an example. Computational complexity involved in real-time control, using the explicit, non- recusive form of equations, is studied on a single CPU and multi- CPU parallel computation processors.

Nomenclature

$q_{2i,j}$ - j^{th} generalized coordinate associated with element $2i$

n_{2i} - number of generalized coordinates associated with element $2i$

$x_{2i,j}, y_{2i,j}, z_{2i,j}$ - j^{th} mode shapes for the deflections of element $2i$ in the x_{2i}, y_{2i}, z_{2i} axes directions, respectively.

W_{2i-1} - homogeneous transformation matrix from coordinate frame to inertial coordinate frame

A_{2i} - homogeneous transformation matrix from coordinate frame $(2i+1)$ to coordinate frame $(2i)$.

K - kinetic energy of the system

P_g - gravitational potential energy

P_e - elastic potential energy

$\mu(\eta_{2i})$ - mass distribution of element

μ_0 - uniform mass distribution value

$\mathbf{q}_1$ - generalized coordinates associated with joint angles between links

$\mathbf{q}_2$ - generalized coordinates associated with link flexibilities

$\mathbf{q}_3$ - generalized coordinates associated with joint flexibilities

m_{2i} - mass of element $2i$ (link i).

E - Young's Modulus of Elasticity of the material

G - Shear Modulus of Elasticity

$(I_x)_{2i}, (I_y)_{2i}, (I_z)_{2i}$ - area moment of inertia of element $2i$ cross section about x_{2i}, y_{2i}, z_{2i} Ωaxes, respectively.

$(A_x)_{2i}$ - cross section area of element $2i$.

$intm$ - maximum rounded integer, i.e: $intm(5.2, 6.3) = 7$

m_{2i-1} - mass of element $2i-1$ (link i).

I_{2i-1} - inertia tensor of element $2i-1$ with respect to a coordinate frame fixed at its center of mass.

$[\ J\ ]$ - generalized inertia matrix of all joints.

g - gravity vector, $[\ g_x, g_y, g_z, 0\ ]^T$

I. Introduction

I. 1. Motivation for the Work

Computer controlled robotic manipulators are very versatile elements of modern flexible manufacturing systems. Their versatility stems from two main characteristics: 1. mechanical reconfigurability, 2. reprogrammability with the control computer. There is an increasing demand for the utilization of robotic manipulators in many manufacturing operations such as milling, grinding, drilling, deburring. Furthermore, manipulators are required to complete their part of job in shorter times, in order to reduce the cycle time and thus improve productivity. This requires manipulators to move faster and faster.

The compliance of the manipulators due to links and joints becomes a significant factor effecting the precision of manipulation, as the manipulator move at high speeds and/or interact with large contact forces. In order to operate within a desired precision range, the computer control algorithms must account for once neglected manipulator compliance. Understanding and appropriately accounting for the compliance in control is a prerequisite for the utilization of manipulators in the forementioned high- performance tasks. Therefore, effective means of modeling the dynamics of manipulators including the link and joint compliance is needed.
In general, there are two different reasons for mathematical modeling of any dynamic system, and for that matter, compliant manipulators.
1. Study and simulate a system before it is actually built. For that purpose, the model should be as accurate and detailed as possible to closely represent (*model*) the actual system, so that the predicted behavior will be close to the actual behavior of the real system.
2. Model only the major characteristics of the system so that it is simple enough to synthesize an appropriate control algorithm, and implement in real-time. Explicit, symbolic form of the flexible manipulator dynamics presented in this paper offers important insights to the dynamic characteristics, which is crucial for the development of an appropriate controller.

1.2. Literature Review

Dynamics and control studies of flexible manipulators have been concentrated on a single joint-single link example [1-3]. The single flexible beam is modeled as a Bernoulli-Euler beam and infinite dimensional vibration coordinates are truncated by a finite number of mode shapes. Joint flexibility is considered as a torsional spring which couples actuator rotor/gear assembly to the link.

Previous work on the Lagrangian formulation based dynamic modeling of multi-link flexible manipulators can be classified into two groups:

1. Lagrangian - Finite Element based methods
2. Lagrangian - Assumed modes based methods.

The small vibration dynamic models of flexible mechanisms and manipulators are developed about a known nominal joint variable trajectories [4]. The coupling effects of deformation coordinates on the joint motions were neglected. This assumption is removed in [5]. Static deflection modes are included in the model in addition to dynamic deflection modes, thus improving the accuracy of model [6]. A two-link flexible arm is modeled with Lagrange- finite element based method, and performance of LQR with prescribed degree of stability is studies [7]. In a recent work, Newton-Euler formulation and Timoshenko beam theory is used [8]. Stiffness matrix accounting for combined flexibility of joints and links is derived for again two-link example [9]. The main advantage of finite element based methods is that the can be applied to complex shaped systems,

covering a wide class of problems. However, the main disadvantage is that they do not give much insight to the dynamic structure of the system.

A general Lagrangian-assumed modes based method is presented in [10]. The equations of motion are developed in recursive form to reduce the real-time computation in inverse dynamic control. A symbolic modeling method based on [10] is developed in [11]. Transfer matrices are used to develop linear frequency domain model of servo controlled manipulators [12]. The method of [10] is more attractive than other methods for the following reasons:

1. It is an easy-to-understand conceptual approach; therefore, utilization of the results by other researchers in the robotics field will be maximum.
2. As a result of using independent set of relative coordinates in kinematic description, dynamic model has a similar form to the rigid manipulator models. Therefore, it provides more insight to the dynamics of the system and may suggest modification of rigid manipulator control algorithms for use on flexible manipulators by exploiting the rigid and flexible manipulator dynamics differences.

II. Problem Statement

Explicit, non-recusive, symbolic modeling of robotic manipulators with compliant links and joints is the problem dealt with in this work. In order to accurately study and simulate the behavior of the system, modeling method should yield accurate models. Yet, simpler models conveying only dominant characteristics of the dynamics are needed for successful controller design. The Lagrangian-assumed modes based method described in [10] fulfill these requirements. Recursive formulation is useful and critically important in computed-torque control. However, the *non-recursive*, direct dynamic form of equations is needed for more general simulation and controller synthesis studies. If the multi-cpu parallel computation is needed in order to implement a detailed dynamic model based controller, the recursive form of equations is not suitable, rather, explicit, non-recursive form is desirable.

III. Symbolic Modeling of Flexible Manipulators

III. 1. Flexible-Arm Kinematic Description

Consider the kinematic structure shown in (Fig.1) representing a manipulator with serial links connected by revolute joints. The elements of the manipulator are numbered, and body fixed moving coordinates are assigned as shown, where O_0XYZ is the inertial coordinate frame. (4x4) homogeneous transformation matrices are used to describe the position and orientation of one coordinate frame with respect to another. Let $\mathbf{q}_{k,j}^T = (q_{k,1}, q_{k,2}, \ldots, q_{k,n_k})$ be the generalized coordinates associated with element k degrees of freedom (d.o.f.). For instance, if element k is a single d.o.f. revolute joint, then $\mathbf{q}_{k,j} = q_{k,1}$, if it is a two d.o.f. revolute joint, then $\mathbf{q}_{k,j} = (q_{k,1}, q_{k,2})^T$. If element k is flexible link, $\mathbf{q}_{k,j}$ is vector of modal coordinates, if the link is rigid (zero d.o.f.), $\mathbf{q}_{k,j}$ is a null vector. The position vector of a differential element along link i (element $2i$) with respect to coordinate frame $2i$ is given by

$$^{2i}h_{2i} = [\,\eta_{2i}, 0, 0, 1\,]^T + \sum_{j=1}^{n_{2i}} q_{2i,j}\,[\,x_{2i,j}, y_{2i,j}, z_{2i,j}, 0\,]^T \qquad (1)$$

The second summation term in (eqn.1) describes the deflection of the element $2i$ at that point in

terms of modal coordinates approximately. The $x_{2i,j}, y_{2i,j}, z_{2i,j}$ are the j^{th} mode shape functions of the element in x_{2i}, y_{2i}, z_{2i} directions, respectively, $q_{2i,j}$ is the generalized modal coordinate, n_{2i} is the number of modes used to describe the deflection of element $2i$. The absolute position of this point with respect to the inertial frame O_0XYZ is given by

$$^0h_{2i}(\eta) = ^0 W_{2i-1} \cdot {}^{2i}h_{2i}(\eta) \tag{2}$$

where $^0W_{2i-1}$ is the (4x4) homogeneous transformation matrix from coordinate frame $2i$ to the inertial coordinate frame (Fig.1)†.

$$W_{2i-1} = A_1 \cdot A_2 \cdots A_{2i-1} \tag{3}$$

Note that if a link is considered rigid, the corresponding link transformation will be a constant matrix. Approximations are involved in the definition of link transformation, A_{2i}, as described below. If link i (element $2i$) were rigid, slender beam, would be (Fig. 2).

$$A_{2i} = \begin{bmatrix} 1 & 0 & 0 & l_{2i} \\ 0 & 1 & 0 & 0 \\ 0 & 0 & 1 & 0 \\ 0 & 0 & 0 & 1 \end{bmatrix} \tag{4}$$

The change in the position and orientation of $(2i+1)^{th}$ coordinate frame due to flexible deflection of link i is described by a differential coordinate transformation (Fig. 2). This is an approximation in the kinematic description. The approximation is valid to the extend that the orientation change of coordinate frame $(2i+1)$ due to deflections is small enough to justify the following approximation:

$$\sin\theta^*_{2i} \simeq \theta^*_{2i}, \qquad \cos\theta^*_{2i} \simeq 1. \tag{5}$$

where θ^*_{2i} is the equivalent rotation angle about an axis of rotation to transform the orientation of $(2i+1)'$ to that of $(2i+1)$. This approximation is well satisfied in robotic applications. Finally, the link transformation A_{2i},

$$A_{2i} = A'_{2i} + dA'_{2i} \tag{6}$$

$$dA'_{2i} = A'_{2i} \cdot {}^{A'_{2i}}\Delta \tag{7}$$

Invoking the modal approximation for the deflections

$$^{A'_{2i}}\Delta = \begin{bmatrix} 0 & -(\theta_z)_{2i} & (\theta_y)_{2i} & x_{2i} \\ (\theta_z)_{2i} & 0 & -(\theta_x)_{2i} & y_{2i} \\ -(\theta_y)_{2i} & (\theta_x)_{2i} & 0 & z_{2i} \\ 0 & 0 & 0 & 0 \end{bmatrix} = \sum_{j=1}^{n_{2i}} q_{2i,j} \begin{bmatrix} 0 & -(\theta_z)_{2i,j} & (\theta_y)_{2i,j} & x_{2i,j} \\ (\theta_z)_{2i,j} & 0 & -(\theta_x)_{2i,j} & y_{2i,j} \\ -(\theta_y)_{2i,j} & (\theta_x)_{2i,j} & 0 & z_{2i,j} \\ 0 & 0 & 0 & 0 \end{bmatrix} \tag{8}$$

Hence

$$A_{2i} = \begin{bmatrix} 1 & 0 & 0 & l_{2i} \\ 0 & 1 & 0 & 0 \\ 0 & 0 & 1 & 0 \\ 0 & 0 & 0 & 1 \end{bmatrix} + \sum_{j=1}^{n_{2i}} q_{2i,j} \begin{bmatrix} 0 & -(\theta_z)_{2i,j} & (\theta_y)_{2i,j} & x_{2i,j} \\ (\theta_z)_{2i,j} & 0 & -(\theta_x)_{2i,j} & y_{2i,j} \\ -(\theta_y)_{2i,j} & (\theta_x)_{2i,j} & 0 & z_{2i,j} \\ 0 & 0 & 0 & 0 \end{bmatrix} \tag{9}$$

†Preceding superscript ^{0} will be dropped for notational simplicity.

A_{2i-1}, (for $i = 1,\ldots,N$), are joint transformations and no approximations involved in their description.

III.2. Flexible-Arm Kinetics: Lagrangian-Assumed Modes Formulation

Once the kinematic description of the system is set up, the next step in Lagrangian formulation is to form the kinetic and potential energies and take the necessary derivatives of the equations of motion:

$$\frac{d}{dt}\left(\frac{\partial K}{\partial \dot{q}_{p,r}}\right) - \frac{\partial K}{\partial q_{p,r}} + \frac{\partial P}{\partial q_{p,r}} = Q_{p,r} \qquad ; \{p = 1,\ldots,2N\,;\ \{r = 1,\ldots,n_p\}\} \tag{10}$$

where

$$K = \sum_{i=1}^{N} K_{2i} \ - \text{ total kinetic energy} \tag{11}$$

$$P = \sum_{i=1}^{N} P_{2i} \ - \text{ total potential energy} \tag{12}$$

$$Q_{p,r} \ - \text{ the generalized force vector} \tag{13}$$

Here only the link dynamics are considered. Inclusion of the joint dynamics into the model will be discussed in Section III.4. Kinetic energy of element $2i$ (link i)

$$K_{2i} = 1/2 \int_0^{l_{2i}} Tr\ \left\{ {}^0\dot{h}_{2i} \cdot {}^0\dot{h}_{2i}{}^T \right\} \mu(\eta)\, d\eta \tag{14}$$

This equation neglects the rotary self-inertias of individual differential elements, which is consistent with the common practice of finite element based formulations.

$${}^0h_{2i}(\eta) = W_{2i-1} \cdot {}^{2i}h_{2i}(\eta) \tag{15}$$

$${}^0\dot{h}_{2i}(\eta) = \dot{W}_{2i-1} \cdot {}^{2i}h_{2i}(\eta) + W_{2i-1} \cdot {}^{2i}\dot{h}_{2i}(\eta) \tag{16}$$

where;

$$\begin{aligned} \dot{W}_{2i-1} &= \sum_{j=1}^{2i-1} \left[A_1 A_2 \ldots \left(\sum_{k=1}^{n_j} \frac{\partial A_j}{\partial q_{j,k}} \right) \ldots A_{2i-1} \right] \dot{q}_{j,k} \\ &= \sum_{j=1}^{2i-1} \sum_{k=1}^{n_j} \left(\frac{\partial W_{2i-1}}{\partial q_{j,k}} \right) \dot{q}_{j,k} \end{aligned} \tag{17}$$

$${}^{2i}\dot{h}_{2i} = \sum_{j=1}^{n_{2i}} \dot{q}_{2i,j} \left[x_{2i,j}, y_{2i,j}, z_{2i,j}, 0 \right]^T \tag{18}$$

Substituting (15 – 18) into (14) and summing over i as in (11) yields the kinetic energy of the manipulator links

$$K = 1/2 \sum_{i=1}^{N} \sum_{s=1}^{2i-1} \sum_{u=1}^{2i-1} \sum_{t=1}^{n_s} \sum_{v=1}^{n_u} Tr \left(\frac{\partial W_{2i-1}}{\partial q_{s,t}} \left[C_{2i} + \sum_{j=1}^{n_{2i}} \left[C_{2i,j} + C_{2i,j}^T \right] q_{2i,j} + \sum_{j=1}^{n_{2i}} \sum_{k=1}^{n_{2i}} C_{2i,j,k}\, q_{2i,j}\, q_{2i,k} \right] \frac{\partial W_{2i-1}^T}{\partial q_{u,v}} \dot{q}_{s,t} \dot{q}_{u,v} \right)$$

$$+ \sum_{i=1}^{N} \sum_{s=1}^{2i-1} \sum_{t=1}^{n_s} Tr \left(\frac{\partial W_{2i-1}}{\partial q_{s,t}} \left[\sum_{j=1}^{n_{2i}} C_{2i,j}\, \dot{q}_{2i,j} + \sum_{j=1}^{n_{2i}} \sum_{k=1}^{n_{2i}} C_{2i,j,k}\, q_{2i,k}\, \dot{q}_{2i,j} \right] W_{2i-1}^T\, \dot{q}_{s,t} \right)$$

$$+ 1/2 \sum_{i=1}^{N} Tr \left(W_{2i-1} \left[\sum_{j=1}^{n_{2i}} \sum_{k=1}^{n_{2i}} C_{2i,j,k}\, \dot{q}_{2i,j}\, \dot{q}_{2i,k} \right] W_{2i-1}^T \right) \tag{19}$$

where;

$$C_{2i} = \int_0^{l_{2i}} [\, \eta_{2i}, 0, 0, 1 \,]^T [\, \eta_{2i}, 0, 0, 1 \,]\, \mu(\eta)\, d\eta \tag{20.a}$$

$$C_{2i,j} = \int_0^{l_{2i}} [\, \eta_{2i}, 0, 0, 1 \,]^T [\, x_{2i,j}, y_{2i,j}, z_{2i,j}, 0 \,]\, \mu(\eta)\, d\eta \tag{20.b}$$

$$C_{2i,j,k} = \int_0^{l_{2i}} [\, x_{2i,j}, y_{2i,j}, z_{2i,j}, 0 \,]^T [\, x_{2i,j}, y_{2i,j}, z_{2i,j}, 0 \,]\, \mu(\eta)\, d\eta \tag{20.c}$$

The potential energy of the system is given by

$$P = P_g + P_e = \sum_{i=1}^{N} [\, (P_g)_{2i} + (P_e)_{2i} \,] \tag{21}$$

The gravitational potential energy, P_g,

$$P_g = \sum_{i=1}^{N} \int_0^{l_{2i}} g^T\, W_{2i-1}\, {}^{2i}h_{2i}(\eta)\, \mu(\eta)\, d\eta \tag{22}$$

Substituting ${}^{2i}h_{2i}$ from (1) into (22)

$$P_g = \sum_{i=1}^{N} g^T\, W_{2i-1} \left[mg_{2i} + \sum_{j=1}^{n_{2i}} q_{2i,j}\, me_{2i,j} \right] \tag{23}$$

where;

$$g^T = [\, g_x, g_y, g_z, 0 \,] = [\, 0, 0, -9.81, 0 \,] \tag{24}$$

$$mg_{2i} = \int_0^{l_{2i}} [\, \eta_{2i}, 0, 0, 1 \,]^T\, \mu(\eta)\, d\eta \tag{25}$$

$$me_{2i,j} = \int_0^{l_{2i}} [\, x_{2i,j}, y_{2i,j}, z_{2i,j}, 0 \,]^T\, \mu(\eta)\, d\eta \tag{26}$$

Incidentally, $me_{2i,j}$ is same as the bottom row of $C_{2i,j}$ in (20.*b*).
Elastic potential energy expression, considering bending in y, z, extension in x, and torsion about x directions, is given by:

$$P_e = \sum_{i=1}^{N} 1/2 \int_0^{l_{2i}} \left\{ E \left[(I_z)_{2i} \left(\frac{\partial^2 z_{2i}}{\partial \eta^2} \right)^2 + (I_y)_{2i} \left(\frac{\partial^2 y_{2i}}{\partial \eta^2} \right)^2 + (A_x)_{2i} \left(\frac{\partial x_{2i}}{\partial \eta} \right)^2 \right] + G (I_x)_{2i} \left(\frac{\partial (\theta_x)_{2i}}{\partial \eta} \right)^2 \right\} d\eta \tag{27}$$

Noting the truncated model approximations for the deformation coordinates of the links (eqn. 1 and 9)

$$P_e = 1/2 \sum_{i=1}^{N} \sum_{j=1}^{n_{2i}} \sum_{k=1}^{n_{2i}} k_{2i,j,k} \quad q_{2i,j} \quad q_{2i,k} \tag{28}$$

where;

$$k_{2i,j,k} = (k_x)_{2i,j,k} + (k_y)_{2i,j,k} + (k_z)_{2i,j,k} + (k_t)_{2i,j,k} \tag{29}$$

$$(k_x)_{2i,j,k} = \int_0^{l_{2i}} E (A_x)_{2i} \left(\frac{\partial x_{2i,j}}{\partial \eta} \right) \left(\frac{\partial x_{2i,k}}{\partial \eta} \right) d\eta \tag{29.a}$$

$$(k_y)_{2i,j,k} = \int_0^{l_{2i}} E (I_y)_{2i} \left(\frac{\partial^2 y_{2i,j}}{\partial \eta^2} \right) \left(\frac{\partial^2 y_{2i,k}}{\partial \eta^2} \right) d\eta \tag{29.b}$$

$$(k_z)_{2i,j,k} = \int_0^{l_{2i}} E (I_z)_{2i} \left(\frac{\partial^2 z_{2i,j}}{\partial \eta^2} \right) \left(\frac{\partial^2 z_{2i,k}}{\partial \eta^2} \right) d\eta \tag{29.c}$$

$$(k_t)_{2i,j,k} = \int_0^{l_{2i}} G (I_x)_{2i} \left(\frac{\partial (\theta_x)_{2i,j}}{\partial \eta} \right) \left(\frac{\partial (\theta_x)_{2i,k}}{\partial \eta} \right) d\eta \tag{29.d}$$

Note that the $k_{2i,j,k}$ term is same structural stiffness values that would be obtained numerically from finite element methods.

III.3. Dynamic Model: Direct Dynamic Form

For general purposes, such as simulation, controller synthesis studies non-recursive dynamic form of the model is needed. For computer-torque (inverse dynamic) control which is a specific control algorithm, the recursive form is desirable [10]. The components of dynamic model should be explicitly separated out to inertial, centrifugal and coriolis, gravitational, and structural stiffness forces terms, so that this information can be embedded in the structure of the real-time control algorithm. For instance, generalized inertia matrix plays a critical role in decoupled joint control of robotic manipulators. In order to implement a real-time decoupled joint controller for a given manipulator, the generalized inertia matrix must be known explicitly so that it can be used in control action calculations. In contrast, the recursive formulation avoids such separations for the sake of least operation needed for inverse dynamic calculations. The non-recursive explicit form of the dynamic model is presented below. If the necessary derivatives are taken and cancellations

are done between the terms Ωgenerated by $\frac{d}{dt}(\partial K/\partial \dot{q}_{p,r})$ and $(\partial K/\partial q_{p,r})$ in eqn(10), and resultant system of equations can be organized in matrix form (30),

$$[M(\mathbf{q})]\ \ddot{\mathbf{q}} + C(\mathbf{q},\dot{\mathbf{q}}) + G(\mathbf{q}) + [K]\ \mathbf{q} = Q \tag{30}$$

where
$\mathbf{q}^T = [(q_{1,1}, q_{1,2}, \ldots, q_{1,n_1}), (q_{2,1}, \ldots, q_{2,n_2}), \ldots, (q_{2N,1}, \ldots, q_{2N,n_{2N}})]$
One row of this matrix equation (30) corresponding to $q_{p,r}$ may be written as;

$$\sum_{s=1}^{2n}\sum_{t=1}^{n_s} m_{(p,r),(s,t)}\ \ddot{q}_{s,t} + C_{(p,r)}(\mathbf{q},\dot{\mathbf{q}}) + G_{(p,r)}(\mathbf{q}) + \sum_{s=1}^{2N}\sum_{t=1}^{n_s} k_{(p,r),(s,t)}\ q_{s,t} = Q_{(p,r)} \tag{31}$$

where

$$(p,r) = \sum_{i=1}^{p-1} n_i + r \qquad \text{– indicating row number and}$$

$$(s,t) = \sum_{i=1}^{s-1} n_i + t \qquad \text{– indicating column number in eqn.(30).}$$

Elements of generalized inertia matrix;

$$m_{(p,r),(s,t)} = {m_{(p,r),(s,t)}}^{(1)} + {m_{(p,r),(s,t)}}^{(2)} + {m_{(p,r),(s,t)}}^{(3)} \tag{32}$$

$${m_{(p,r),(s,t)}}^{(1)} = \sum_{\substack{i=intm \\ (\frac{p+1}{2},\frac{s+1}{2})}}^{N} Tr\left(\frac{\partial W_{2i-1}}{\partial q_{s,t}}\left[C_{2i} + \sum_{j=1}^{n_{2i}}[C_{2i,j} + C_{2i,j}^T]\,q_{2i,j} + \sum_{j=1}^{n_{2i}}\sum_{k=1}^{n_{2i}} C_{2i,j,k}\,q_{2i,j}\,q_{2i,k}\right]\frac{\partial W_{2i-1}^T}{\partial q_{p,r}}\right) \tag{32.a}$$

$${m_{(p,r),(s,t)}}^{(2)} = Tr\left(\frac{\partial W_{s-1}}{\partial q_{p,r}}[C_{s,t} + \sum_{k=1}^{n_s} C_{s,t,k}\ q_{s,k}]\,W_{s-1}^T\right) \tag{32.b}$$

$${m_{(p,r),(s,t)}}^{(3)} = \begin{cases} W_{p-1}\ C_{p,r,t}\ W_{p-1}^T & ;\ s = p \\ 0 & ;\ s \neq p \end{cases} \tag{32.c}$$

Elements of nonlinear centrifugal and coriolis terms vector;

$$C_{(p,r)}(\mathbf{q},\dot{\mathbf{q}}) =$$

$$\sum_{\substack{i=intm \\ (\frac{p+1}{2},\frac{s+1}{2})}}^{N} \sum_{s=1}^{2i-1} \sum_{u=1}^{2i-1} \sum_{t=1}^{n_s} \sum_{v=1}^{n_u} Tr\left(\frac{\partial^2 W_{2i-1}}{\partial q_{s,t} \partial q_{u,v}} \left[C_{2i} + \sum_{j=1}^{n_{2i}} [C_{2i,j} + C_{2i,j}^T]\, q_{2i,j} + \sum_{j=1}^{n_{2i}} \sum_{k=1}^{n_{2i}} C_{2i,j,k}\, q_{2i,j}\, q_{2i,k} \right] \frac{\partial W_{2i-1}^T}{\partial q_{p,r}} \dot{q}_{s,t}\, \dot{q}_{u,v} \right)$$

$$+ \sum_{\substack{i=intm \\ (\frac{p+1}{2},\frac{s+1}{2})}}^{N} \sum_{s=1}^{2i-1} \sum_{t=1}^{n_s} Tr\left(\frac{\partial W_{2i-1}}{\partial q_{p,r}} \left[2 \sum_{j=1}^{n_{2i}} C_{2i,j}\, \dot{q}_{2i,j} + 2 \sum_{j=1}^{n_{2i}} \sum_{k=1}^{n_{2i}} C_{2i,j,k}\, q_{2i,k}\, \dot{q}_{2i,j} \right] \frac{\partial W_{2i-1}^T}{\partial q_{s,t}} \dot{q}_{s,t} \right)$$

$$+ \sum_{s=1}^{p-1} \sum_{t=1}^{n_s} \sum_{u=1}^{p-1} \sum_{v=1}^{n_u} Tr\left(\frac{\partial^2 W_{2i-1}}{\partial q_{s,t} \partial q_{u,v}} \left[C_{p,r} + \sum_{k=1}^{n_p} C_{p,r,k}\, q_{p,k} \right] W_{p-1}^T\, \dot{q}_{s,t}\, \dot{q}_{u,v} \right)$$

$$+ \sum_{s=1}^{p-1} \sum_{t=1}^{n_s} Tr\left(\frac{\partial W_{p-1}}{\partial q_{s,t}} \left[2 \sum_{k=1}^{n_p} C_{p,r,k}\, \dot{q_{p,k}} \right] W_{p-1}^T\, \dot{q_{s,t}} \right) \tag{33}$$

Elements of the gravity vector

$$G_{(p,r)}(\mathbf{q}) = \sum_{\substack{i=intm \\ (\frac{p+1}{2},\frac{s+1}{2})}}^{N} g^T \frac{\partial W_{2i-1}}{\partial q_{p,r}} \left[m g_{2i} + \sum_{j=1}^{n_{2i}} me_{2i,j}\, q_{2i,j} \right] + g^T W_{p-1}\ me_{p,r} \tag{34}$$

Elements of structural stiffness matrix

$$k_{(p,r),(s,t)} = \begin{cases} k_{p,r,t} & \text{for } p = s \\ 0 & \text{for } p \neq s \end{cases} \tag{35}$$

Note some simplifying fact as follows:

$$C_{p,r},\ C_{p,r,k},\ k_{p,r,t} = 0 \qquad \text{for} \quad p - \text{odd} \tag{36.a}$$

$$\frac{\partial W_{s-1}}{\partial q_{p,r}} = 0 \qquad \text{for} \quad s - 1 < p \tag{36.b}$$

In symbolic expansion of eqns. (32) through (35) for a manipulator, these facts ($36.a - -36.b$) will be automatically utilized and will cancel out the terms that are already known to be zero. Such capabilities are conveniently provided by commercial symbolic manipulation programs (SMP, MACSYMA, REDUCE).

Considering the facts (35) - (36), and rearranging generalized coordinate vector into two groups associated with joint and link flexibility.

$$[\, \mathbf{q}_1^T, \mathbf{q}_2^T \,] = [\, (q_{1,j}, q_{3,j}, \ldots.)^T, (q_{2,j}, q_{4,j}, \ldots.)^T \,] \tag{37}$$

The equations of motion (30) can be shown to have the following form:

$$\begin{bmatrix} m_r & m_{rf} \\ m_{rf}^T & m_f \end{bmatrix} \begin{Bmatrix} \ddot{\mathbf{q}}_1 \\ \ddot{\mathbf{q}}_2 \end{Bmatrix} + \begin{Bmatrix} C_1(\mathbf{q}_1, \mathbf{q}_2, \dot{\mathbf{q}}_1, \dot{\mathbf{q}}_2) \\ C_2(\mathbf{q}_1, \mathbf{q}_2, \dot{\mathbf{q}}_1, \dot{\mathbf{q}}_2) \end{Bmatrix} + \begin{Bmatrix} G_1(\mathbf{q}_1, \mathbf{q}_2) \\ G_2(\mathbf{q}_1, \mathbf{q}_2) \end{Bmatrix} + \begin{bmatrix} 0 & 0 \\ 0 & K_f \end{bmatrix} \begin{Bmatrix} \mathbf{q}_1 \\ \mathbf{q}_2 \end{Bmatrix} = \begin{Bmatrix} \mathbf{u} \\ 0 \end{Bmatrix} \tag{38}$$

III.4. Inclusion of Joint Dynamics

Inclusion of joint dynamics into model involves

1. modifications of eqn. $(20.a-c)$, (25), and (26) by redefining mass distribution of links,
2. augmenting a set of second order equations to (38) as a result of joint flexibility and inertia.

DC motor-driven revolute joints whose rotor/gear arrangement is elastically coupled to the links will be considered. Joints can have more than one degree of freedom. Elastic mechanical coupling between a joint and link is modeled as a torsional spring. The following assumptions are made regarding the joint assembly mass distribution.

Assumption 1: Rotational kinetic energy of each joint about its own center of mass is only due to its own rotation. Rotational kinetic energy due to rotation of previous joints and links is neglected. This amounts to neglecting terms in the order of gear reduction ratio, which is typically in the order of 1 : 100. Translational kinetic energy due to both previous joints and elastic deformations is taken into account.

Assumption 2: Rotor/gear assembly inertia is symmetric about the rotor axis of rotation such that gravitational potential energy, and translational velocity of joint center of mass are independent of rotor position [3]. This assumption is generally satisfied by joint assemblies of most industrial robots.

Let $\mathbf{q}_3^T = [(q_{1,1}^{(j)},...,q_{1,n_1}^{(j)}),(q_{3,1}^{(j)},...,q_{3,n_3}^{(j)}),.....(q_{2N-1,1}^{(j)},....,q_{2N-1,n_{2N-1}}^{(j)})]$

be the generalized coordinates associated with joints (Fig. 3). The relative motion between a joint rotor and elastically coupled link is $(q_{2i-1,r} - q_{2i-1,r}^{(j)})$. The contribution of the joint dynamics to the equation of motion will be reflected through kinetic, potential energies and generalized forces. The kinetic energy of joint i (element $2i-1$) is

$$K_{2i-1} = 1/2\ m_{2i-1}\ (V_G)_{2i-1}^T \cdot (V_G)_{2i-1}\ +\ 1/2\ w_{2i-1}^T\ [I_{2i-1}]\ w_{2i-1} \tag{39}$$

where m_{2i-1} is the mass, $(V_G)_{2i_1}$ velocity of center of mass, w_{2i-1} angular velocity vector, $[I_{2i-1}]$ inertia tensor with respect to a coordinate frame fixed at the center of mass of joint. From assumption 2, $(V_G)_{2i-1}$ will be function of the generalized coordinates of proximal elements and will not depend on $q_{2i-1,r}^{(j)}$. Therefore, translational kinetic energy of joint i can be included in the formulation by considering its mass as part of the proximal link. This is accomplished by redefining mass distribution of link $(i-1)$ as

$$\mu_{2i-2} = \mu_0 + m_{2i-1}\quad \delta(\eta - l_{2i-2}) \tag{40}$$

where

$$\delta(\eta - l_{2i-2}) = \begin{cases} 1 & \text{for } \eta = l_{2i-2} \\ 0 & \text{for } \eta \neq l_{2i-2} \end{cases} \tag{41}$$

and evaluate eqn.$(20.a-c)$ with new definition of μ as in (40).
From assumption 1, $w_{2i-1} \approx \dot{q}_{2i-1,r}^{(j)}$

$$K_{2i-1} = 1/2\ (\dot{q}_{2i-1,r}^{(j)})^T\quad [I_{2i-1}]\quad \dot{q}_{2i-1,r}^{(j)} \tag{42}$$

For all joints of the manipulator

$$K^{(j)} = \sum_{\substack{i=intm \\ (\frac{p+1}{2},\frac{s+1}{2})}}^{N} K_{2i-1} = 1/2\ \dot{\mathbf{q}}_3^T\ [J]\ \dot{\mathbf{q}}_3 \tag{43}$$

The contribution of joint potential energy to the dynamic model equations

$$V^{(j)} = V_g^{(j)} + V_e^{(j)} \tag{44}$$

From assumption 2, the gravitational potential energy of joint i may be included in that of link $(i-1)$ by the evaluation of (25) and (26) with $\mu(\eta)$ as defined in eqn(40). The elastic potential energy stored in elastic coupling between joint and links

$$V_e^{(j)} = 1/2\ (\mathbf{q}_1 - \mathbf{q}_3)^T\ Diag\{K_t\}\ (\mathbf{q}_1 - \mathbf{q}_3) \tag{45}$$

As a result of the contributions of (43) and (45) equations of motion (38) is modified to the following form:

$$\begin{bmatrix} m_r & m_{rf} \\ m_{rf}^T & m_f \end{bmatrix} \begin{Bmatrix} \ddot{\mathbf{q}}_1 \\ \ddot{\mathbf{q}}_2 \end{Bmatrix} + \begin{Bmatrix} C_1(\mathbf{q}_1, \mathbf{q}_2, \dot{\mathbf{q}}_1, \dot{\mathbf{q}}_2) \\ C_2(\mathbf{q}_1, \mathbf{q}_2, \dot{\mathbf{q}}_1, \dot{\mathbf{q}}_2) \end{Bmatrix} + \begin{Bmatrix} G_1(\mathbf{q}_1, \mathbf{q}_2) \\ G_2(\mathbf{q}_1, \mathbf{q}_2) \end{Bmatrix} + \begin{bmatrix} 0 & 0 \\ 0 & K_f \end{bmatrix} \begin{Bmatrix} \mathbf{q}_1 \\ \mathbf{q}_2 \end{Bmatrix} = \begin{bmatrix} K_t & 0 \\ 0 & 0 \end{bmatrix} \begin{Bmatrix} \mathbf{q}_1 - \mathbf{q}_3 \\ \mathbf{q}_2 \end{Bmatrix}$$

$$[J]\{\ddot{\mathbf{q}}_3\} + [K_T]\{\mathbf{q}_3 - \mathbf{q}_1\} = \{\ \mathbf{u}\} \tag{46a,b}$$

IV. A Case Study

The described modeling method is applied to a two-link planar flexible arm, with single d.o.f revolute joints (Fig. 4). In this case study, only the link flexibilities are considered, the joint flexibilities are not included. The bending deflections of links are approximated with two assumed mode shapes for each link. Mode shapes are chosen from the analytical solution of a Euler- Bernoulli beam eigenfunction analysis but, of course, could also be obtained using a finite element analysis program. The mathematical model is symbolically obtained using SMP symbolic manipulation program and simulated with a VAX-11/750 microcomputer with the following objectives:

1. Verify that the model generated by the above algorithm is correct
2. Demonstrate the ease of changing mode shapes for the given example manipulator, and study the effect of using different mode shapes on the predicted dynamic response of the system.

Model verification is supported by comparing the response of the flexible arm model with that of rigid arm model. Clearly, as the flexural rigidity, EI_z , of the links increase, joint angle response of flexible model should converge to that of rigid model. This is observed as shown in Fig. 5 and Fig. 6.a,b. In simulations of Fig. 6, mode shapes corresponding to clamped-free boundary conditions of a beam were used in the model. Now, let us consider the case that one would like to use a different set of mode shapes. The necessary change required in the model is to re-evaluate the following terms with new mode shapes (considering the fact that selected mode shapes form an orthogonal set): $\{\ C_{2i,j}, C_{2i,j,k}, K_{2i,j,k}$ for $i = 1, 2$ and $j = k = 1, 2$: $(C_{2,1}, C_{2,2}, C_{4,1}, C_{4,2}), (C_{2,1,1}, C_{2,2,2}, C_{4,1,1}, C_{4,2,2}), (K_{2,1,1}, K_{2,2,2}, K_{4,1,1}, K_{4,2,2})\ \}$, $me_{2i,j}$ must be updated with the new values of forth row of $C_{2i,j}$. Fig. 7a-b show the same simulation case results of flexible model with clamped-clamped mode shapes. The reason for faster convergence of joint

angle responses to those of rigid model is that clamped-clamped modes shape results in a stiffer model than clamped-free mode shapes.

Computational complexity of the resultant model is studied for real-time dynamic control of flexible manipulators. These computational results give us an idea about the algebraic complexity of the explicitly symbolic model and the computational power need for real-time control. Since we have obtained the equations in explicit, symbolic form, we could simply equally distribute the computational load over a multi-CPU architecture where each processor could work independent of each other. The computation time for the inverse dynamics of the example flexible manipulator (Fig. 4) is as follows:

1. Computer: VAX-11/750
   a) without floating point accelerator: $7\,Hz$.
   b) with floating point accelerator: $14\,Hz$.
2. Computer: 8 transputer (T414) configured in parallel computation architecture (estimated value, not fully implemented): $80\,Hz$.

It seems that real-time dynamic control of large dimensional flexible systems can only be realized by distributing the real-time computation load over an array of processors, for the dynamic model equations are, in general, too complicated to be handled by a single processor at a fast enough rate for real-time control. Explicit non-recursive form of equations readily lends itself for multi-CPU implementation. This is not possible using recursive form of model.

V. Summary and Conclusion

The elastic deformations are described by summation of a finite number of mode shapes which may either be assumed or obtained from a finite element analysis program. Link deformations are assumed to be small enough to justify differential coordinate transformation and linear elasticity theory (eqn. 6 – 9, and 27).
The modeling method considers all dynamic couplings (linear and nonlinear) between deflection and joint coordinates. Links are assumed to be slender beams. Revolute joints with multiple degrees of freedom are allowed. Joint flexibility as well as link flexibility are included.

Explicit symbolic form of the equations are directly useful for simulation and control studies. Computer automated symbolic expansion of equations (32 - 35, and 46) to obtain dynamic model for any desired manipulator structure is studied and an example case is presented. Dynamic model is presented in an analogous way to the dynamic model of rigid manipulators. This displayed the way link and joint flexibility enter the model, i.e. $C_{2i,j}, C_{2i,j,k}$ terms in the elements of generalized inertia matrix. The mode shape dependent model parameters are identified and changing mode shapes for a given model is simplified (only $C_{2i,j}, C_{2i,j,k}, K_{2i,j,k}$ need to be re-evaluated for new mode shapes).
Explicit symbolic modeling method presented here has the following advantages:

1. improves the insightful understanding of dynamics of flexible manipulators.
2. often equations must be simplified for real-time control implementation. The importance of each term can be determined by simulations and simply wipe off the non-major terms in the symbolic equations.
3. equations readily lend themselves for multi-CPU parallel computation for real- time control.
4. changing mode shapes for a given model is very simple.
5. the approach is conceptually easy-to-understand and similar to rigid manipulator formulations.

Acknowledgments

This work was supported in part by the National Aeronautics and Space Administration under grant NAG-1-623, and the National Science Foundation under grant MEA-8303539.

References

1. Hastings, G.G., Book, W.J., "Verification of a Linear Dynamic Model for Flexible Robotic Manipulators", *IEEE Control Systems Magazine, IEEE Control Systems Society*, April, 1987.

2. Cannon, R.H.Jr., Schmitz, E., "Initial Experiments on the End-Point Control of a Flexible One-Link Robot", *The International Journal of Robotics Research*, Vol. 3, No. 3, Fall 1984, pp. 62- 75.

3. Spong, M.W., "Modeling and Control of Elastic Joint Robots", *Trans. of ASME, J. of Dyn. Sys. Mea. and Control*, Vol. 109, Dec. 1987, pp. 310-319.

4. Sunada, W., Dubowsky, S., "On the Dynamic Analysis and Behavior of Industrial Robotic Manipulators with Elastic Members", *Transactions of ASME, J. Mech.,Trans., Automation and Design*, Vol 105, 1983, pp. 42-51.

5. Shabana, A.A., Wehage, R.A., "A coordinate Reduction Technique for Dynamic Analysis of Spatial Substructures with Large Angular Rotations", *J.Struct. Mech.*, 1983, pp. 401-431.

6. Yoo, W.S., Haug, E.J., "Dynamics of Flexible Mechanical Systems" , *Third Army Conference on Applied Mathematics and Computing*, May 13-16, 1985 , Atlanta , Georgia.

7. Usoro, P.B., Nadira, R.,Mahil, S.S., "Advanced Control of Flexible Manipulators", *Phase I Final report*, NSF Award Number ECS-8260419, April 1983.

8. Naganathan, G., Soni, A.H., " Coupling Effects of Kinematics and Flexibility in Manipulators", *The International Journal of Robotics Research*, Vol. 6, No. 1, Spring 1987, pp. 75-84.

9. Shahinpoor, M., Meghdari, A., "Combined flexural-joint stiffness matrix and elastic deformation of a servo-controlled two-link robot manipulator", *Robotica*, Vol. 4, 1986, pp. 237-242.

10. Book, W.J., "Recursive Lagrangian Dynamics of Flexible Manipulator Arms", *International Journal of Robotic Research*, Vol. 3, No. 3, Fall 1984, pp.87-101.

11. Book, W.J., Majette, M., "Controller Design for Flexible, Distributed Parameter Mechanical Arms Via Combined State Space and Frequency Domain Techniques", *Journal of Dynamic Systems, Measurement, and Control* , Vol. 105, Dec. 1985, pp.245-254.

12. Cetinkunt, S., Book, W.J., "Symbolic Modeling of Flexible Manipulators", *Proc. of 1987 IEEE International Conf. on Robotics and Automation*, March 31- April 3, 1987, Raleigh, NC., Vol. 3, pp. 2074-2080.

13. Leu, M.C., Hemati, N., "Automated Symbolic Derivation of Dynamic Equations of Motion for Robotic Manipulators", *Journal of Dynamic Systems, Measurement, and Control*, Vol.108, Sept. 1986, pp. 172-179.

14. Neuman, C.P., Murray, J.J., "The Complete Dynamic Model and Customized Algorithms of the Puma Robot", *IEEE Trans. on System, Man, and Cybernetics*, Vol. SMC-17, No. 4, July/August 1987, pp. 635-644.

List of Figures

Fig. 1 - Kinematic description of serial link flexible manipulators

Fig. 2 - Illustration of flexible link transformation

Fig. 3 - Flexible joint-link assembly.

Fig. 4 - Two-link flexible manipulator example.

Fig. 5 - Two-link rigid model joint angle responses.

Fig. 6 - Two-link flexible model joint angle responses– Clamped- free mode shapes:

(a) $EI_i = 10\,Nt\,m^2$
(b) $EI_i = 100\,Nt\,m^2$

Fig. 7 - Two-link flexible model joint angle responses – Clamped- clamped mode shapes:

(a) $EI_i = 10\,Nt\,m^2$,
(b) $EI_i = 100\,Nt\,m^2$

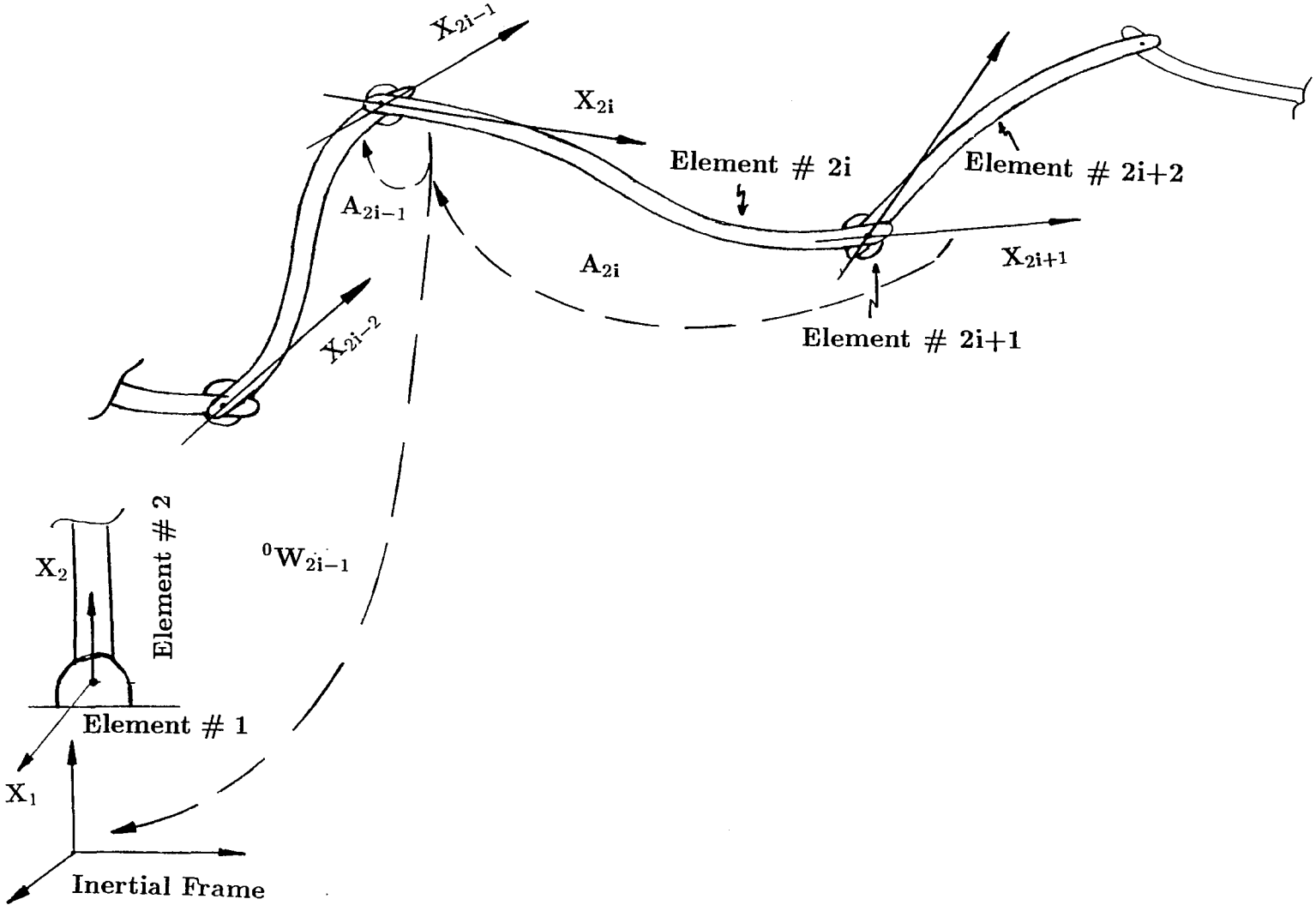
X_{2i-1}
X_{2i}
Element # 2i
Element # 2i+2
A_{2i-1}
A_{2i}
X_{2i+1}
X_{2i-2}
Element # 2i+1
Element # 2
X_2
${}^0W_{2i-1}$
Element # 1
X_1
Inertial Frame

Fig. 1

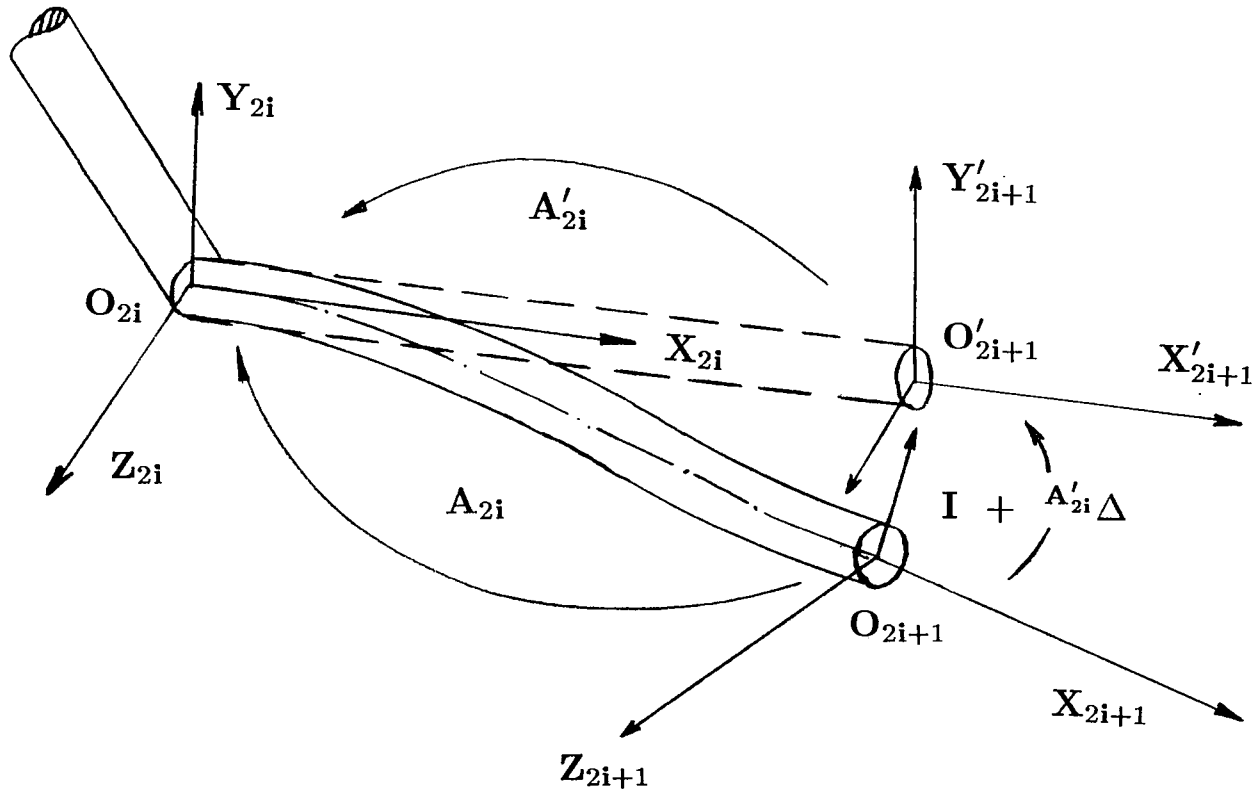
Y_{2i}
A'_{2i}
Y'_{2i+1}
O_{2i}
X_{2i}
O'_{2i+1}
X'_{2i+1}
Z_{2i}
A_{2i}
$I + A'_{2i}\Delta$
O_{2i+1}
X_{2i+1}
Z_{2i+1}

Fig. 2

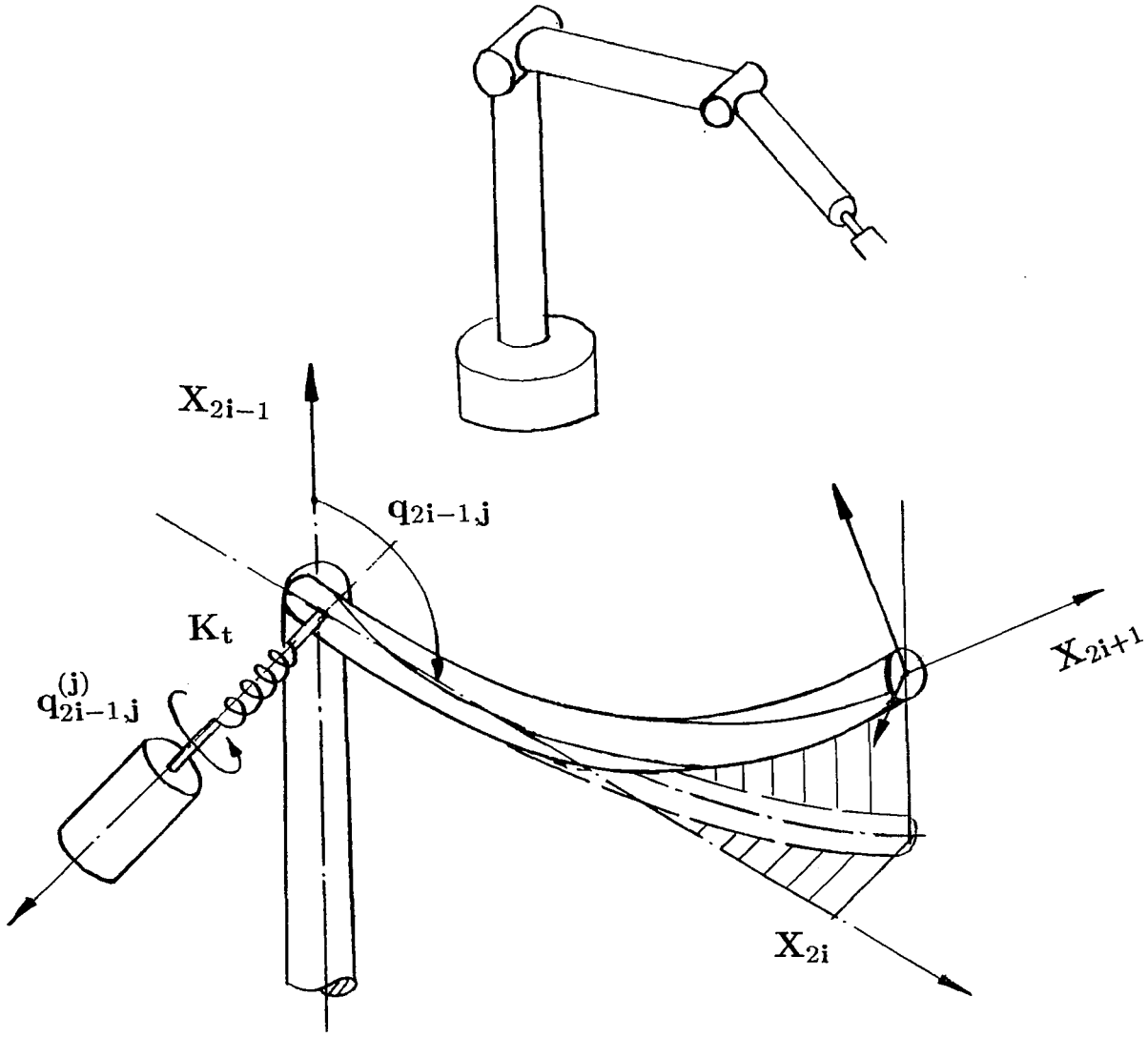

Fig. 3

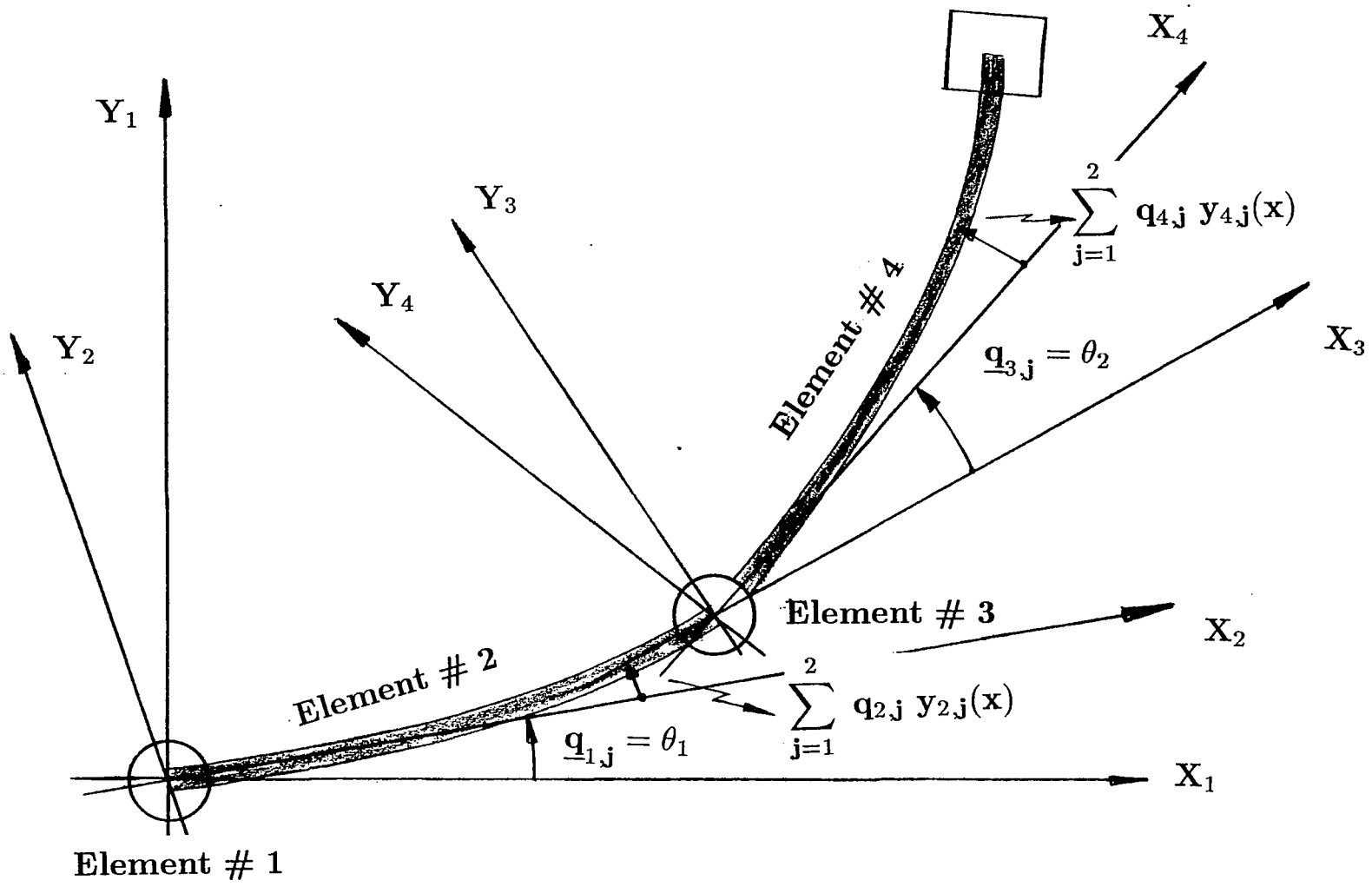
Y_1
Y_2
Y_3
Y_4
X_4
X_3
X_2
X_1
$\sum_{j=1}^{2} q_{4,j}\, y_{4,j}(x)$
$\underline{q}_{3,j} = \theta_2$
$\sum_{j=1}^{2} q_{2,j}\, y_{2,j}(x)$
$\underline{q}_{1,j} = \theta_1$
Element # 1
Element # 2
Element # 3
Element # 4

Fig. 4

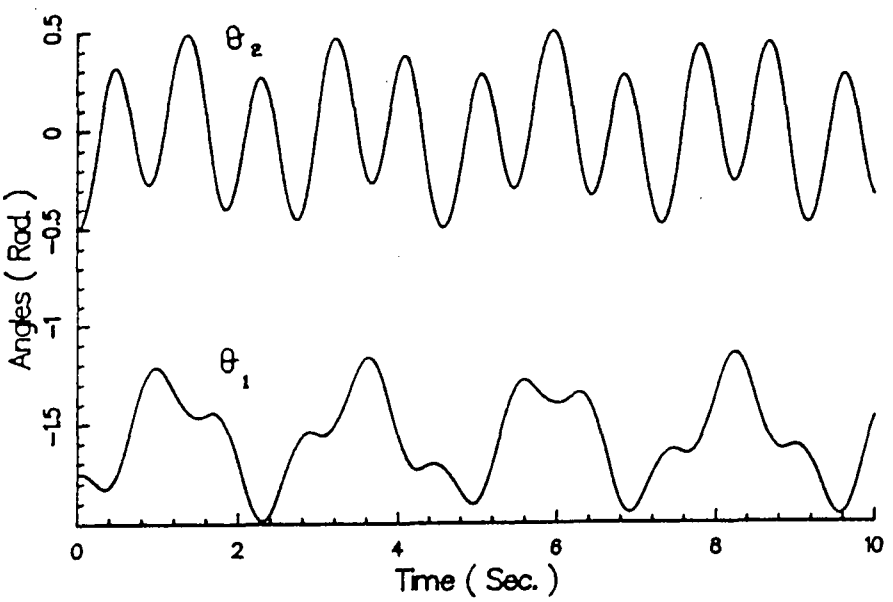

Fig. 5

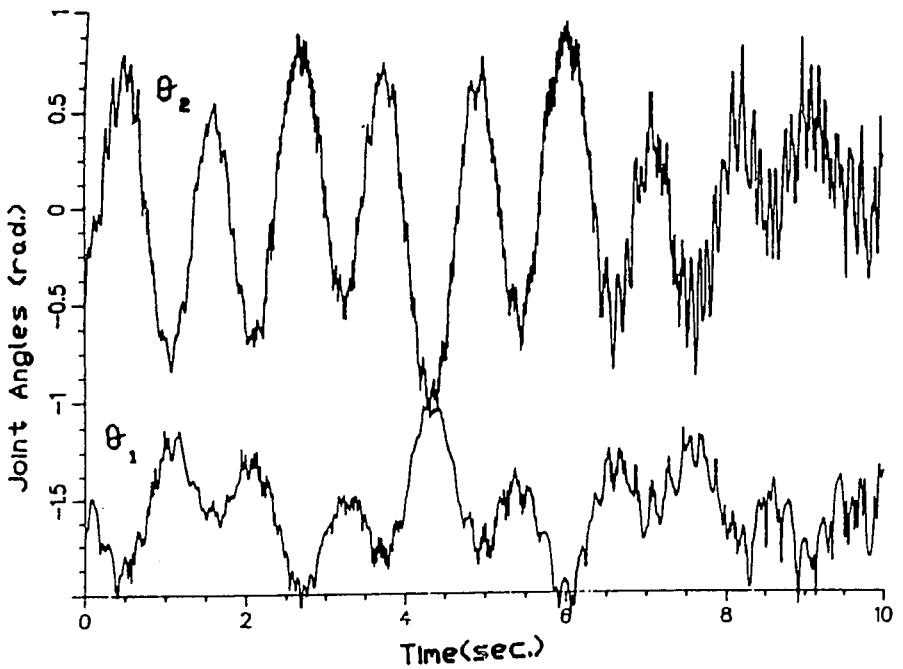
Joint Angles (rad.)
θ2
θ1
1
0.5
0
-0.5
-1
-1.5
0
2
4
6
8
10
Time(sec.)

(a)

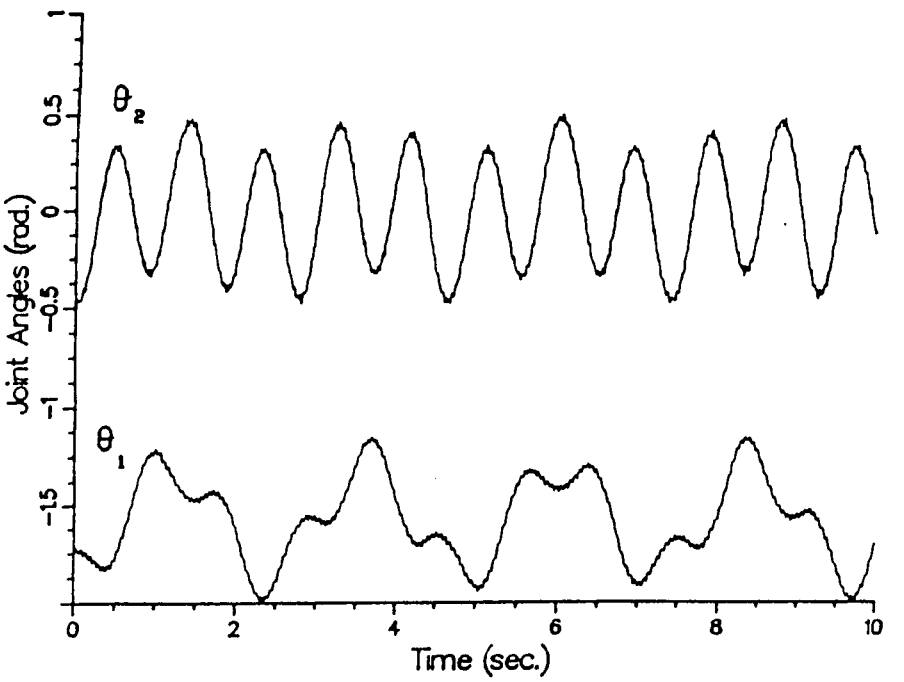
Joint Angles (rad.)
θ2
θ1
1
0.5
0
-0.5
-1
-1.5
0
2
4
6
8
10
Time (sec.)

(b)

Fig. 6

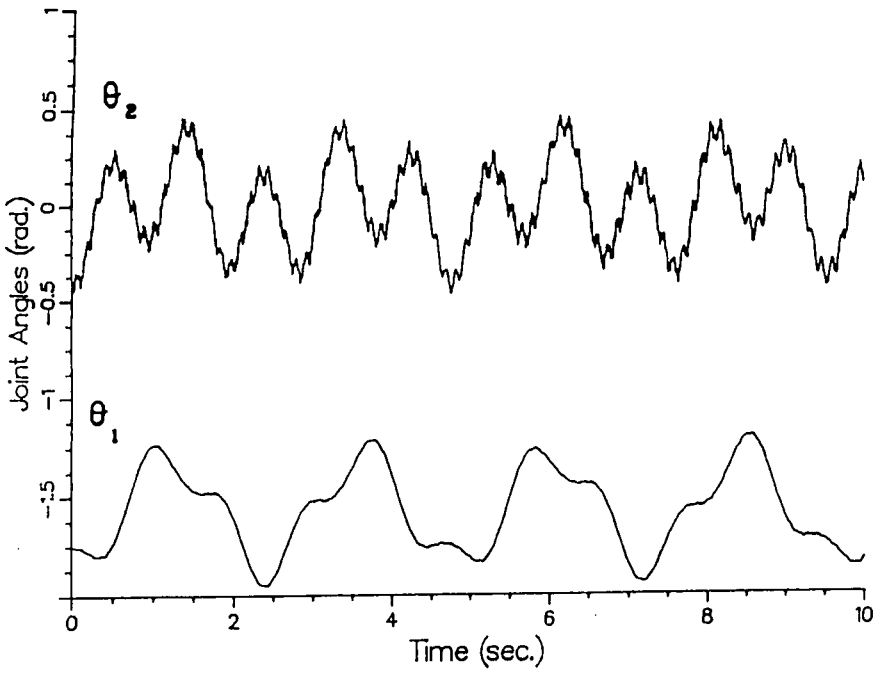
θ2
θ1
Joint Angles (rad.)
1
0.5
0
-0.5
-1
-1.5
0
2
4
6
8
10
Time (sec.)

(a)

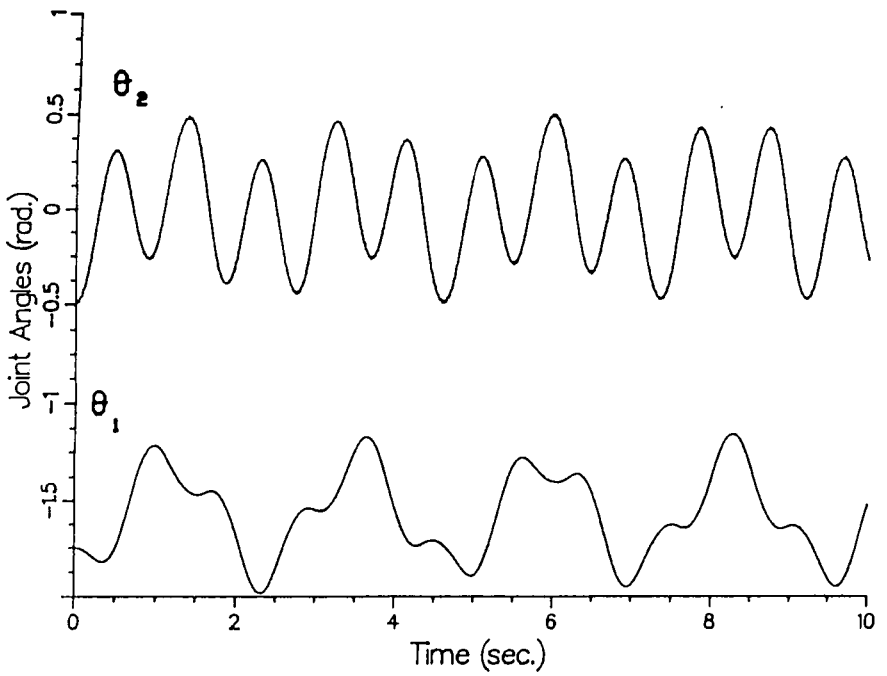
θ2
θ1
Joint Angles (rad.)
1
0.5
0
-0.5
-1
-1.5
0
2
4
6
8
10
Time (sec.)

(b)

Fig. 7